Environmental Modelling and Software 109 (2018) 152–166

Contents lists available at ScienceDirect

Environmental Modelling & Software

journal homepage: www.elsevier.com/locate/envsoft

Do salt marshes survive sea level rise? Modelling wave action, morphodynamics and vegetation dynamics

Ü.S.N. Best[a,d,*], M. Van der Wegen[a,b], J. Dijkstra[b], P.W.J.M. Willemsen[b,c,e,f], B.W. Borsje[c,g], Dano J.A. Roelvink[a,b,d]

[a] Coastal Systems, Engineering & Port Development Chair Group, IHE-Delft Institute for Water Education, PO Box 3015, 2601 DA, Delft, the Netherlands
[b] Deltares, P.O. Box 177, 2600 MH, Delft, the Netherlands
[c] People, Marine & Fluvial Systems Chair Group, University of Twente, PO BOX 217, 7500 AE, Enschede, the Netherlands
[d] Department of Hydraulic Engineering, TU Delft University of Technology, Postbus 5, 2600 AA, Delft, the Netherlands
[e] Department of Estuarine and Delta Systems, Netherlands Institute for Sea Research (NIOZ), PO Box 59, 1790 AB, Den Burg, the Netherlands
[f] Utrecht University, P.O. Box 140, 4400 AC, Yerseke, the Netherlands
[g] Board Young Waddenacademie, Ruiterskwartier 121a, 911 BS, Leeuwarden, the Netherlands

ARTICLE INFO

Keywords:
Salt marshes
Mudflats
Bio-geomorphology
Sea level rise (SLR)
Waves
Mud-morphodynamics

ABSTRACT

This paper aims to fundamentally assess the resilience of salt marsh-mudflat systems under sea level rise. We applied an open-source schematized 2D area model (Delft3D) that couples intertidal flow, wave-action, sediment transport, geomorphological development with a population dynamics approach including temporal and spatial growth of vegetation and bio-accumulation. Wave-action maintains a high sediment concentration on the mudflat while the tidal motion transports the sediments within the vegetated marsh areas during flood. The marsh-mudflat system attained dynamic equilibrium within 120 years. Sediment deposition and bio-accumulation within the marsh make the system initially resilient to sea level rise scenarios. However, after 50–60 years the marsh system starts to drown with vegetated-levees being the last surviving features. Biomass accumulation and sediment supply are critical determinants for the marsh drowning rate and survival. Our model methodology can be applied to assess the resilience of vegetated coast lines and combined engineering solutions for long-term sustainability.

1. Introduction

Traditionally, the approaches to coastal defence have utilized structural measures to ensure a desired level of safety for the surrounding areas. This concept has been instrumental for coastal management strategies around the world to ensure the protection of low-lying regions against the imminent threat of inundation. However, not only has this measure resulted in dire impacts on local ecology and surrounding ecosystems (Airoldi et al., 2005), but it appears not so sustainable in combating the scenarios with Sea Level Rise (SLR). Instead, innovative solutions could be implemented that comprise a combination of both structural and non-structural measures. One such non-structural measure builds on the 'Building with Nature' concept for the reduction of risk due to inundation and proposes the use of vegetated foreshores (Borsje et al., 2011; Temmerman et al., 2013; Vuik et al., 2016).

The growth of vegetation, serves several ecosystem services that are pertinent toward flood management strategies. The establishment of vegetation on the mudflat, initially in patches, results in the concentration of flows with a subsequent increase in bed shear stresses and the initiation of channels (Balke et al., 2013; Hu et al., 2015; Schwarz et al., 2011; Temmerman et al., 2003; Temmerman et al., 2010). Channels are known to ensure the drainage, growth and expansion of the intertidal vegetation (Attema, 2014; Mudd and Fagherazzi, 2016; Stark et al., 2017). The expansion of the vegetation patches coupled with the ability of the vegetation to capture and trap sediments have led to the development of stable salt marsh-mudflat systems (Bendoni et al., 2016; Fagherazzi et al., 2012; Kirwan et al., 2016; Maan et al., 2015; Schepers et al., 2017). These stable systems reduce the magnitude of the tidal currents, wave action and associated erosion patterns in bare

* Corresponding author. Coastal Systems, Engineering & Port Development Chair Group, IHE-Delft Institute for Water Education, PO Box 3015, 2601 DA, Delft, the Netherlands.
E-mail addresses: u.best@un-ihe.org (Ü.S.N. Best), m.vanderwegen@un-ihe.org (M. Van der Wegen), Jasper.Dijkstra@deltares.nl (J. Dijkstra), p.willemsen@utwente.nl (P.W.J.M. Willemsen), b.w.borsje@utwente.nl (B.W. Borsje), d.roelvink@un-ihe.org (D.J.A. Roelvink).

https://doi.org/10.1016/j.envsoft.2018.08.004
Received 6 September 2017; Received in revised form 18 April 2018; Accepted 3 August 2018
Available online 10 August 2018

mudflats (Bendoni et al., 2016; Tonelli et al., 2010). Moreover, these vegetated systems are existing features which are instrumental for low-lying countries that are experiencing the effects of SLR: higher spring tides, larger waves, increased overtopping frequencies and the loss of kilometres of foreshores, among others (Trenhaile, 2009).

However, according to Bouma et al. (2016), salt marsh systems are prone to erosion and accretion (years), attributed to a decrease in sediment supply and increases in the magnitude of the wave action and the frequency of extreme events (Allen, 2000; Cowell and Thom, 1995; Mariotti and Fagherazzi, 2010; Schwimmer, 2001; Stark et al., 2017; Vuik and Jonkman, 2016). Pressures may also extend to the competition stresses induced within and among plant species, and to human interventions for protection and reclamation purposes. The erosion process may result in a substantial loss of the intertidal vegetation cover, leaving low-lying sections of the foreshore open to the full impact of the waves and tidal surges (Temmerman et al., 2005; Temmerman et al., 2010; Thampanya et al., 2006). The effects of these triggers are made visible through the lateral dynamics of the marsh and the rate at which the marsh heightens and may have lasting impacts on the ecology of the system (Maan et al., 2015; Mudd et al., 2010; Nyman et al., 2006).

Intertidal marsh-mudflat areas are under tremendous pressure from SLR. By the year 2100, mean sea water level may realize increases ranging from 0.6 m to 1.1 m (IPCC, 2013; Schile et al., 2014; Stocker, 2014). Studies have shown that the system's sediment balance both internally and externally, may enable it to adjust the bed level at a rate that matches SLR (Winterwerp et al., 2013). However, if the system is unable to timely adjust, this will trigger a landward retreat of the vegetation as they are displaced to available areas of a higher elevation. Mudflats may drown under SLR scenarios providing less sediments to adjacent salt marshes (Van der Wegen and Roelvink, 2008). Additionally, when space is limited landward due to the construction of dykes or seawalls, the vegetation is trapped between the prograding high water line and the obstacles. This coastal squeeze results in the vegetation being unable to survive extensive durations of inundation (Bouma et al., 2016). Definite conclusions on the long-term resilience (i.e. magnitude and extent) of salt marsh mudflat systems under SLR scenarios are to date uncertain (Clough et al., 2016; Crosby et al., 2016; Schile et al., 2014).

The feedbacks between the plant growth and the geomorphological developments are known to trigger increases in the bed level due to the accumulation of organic and mineral components at a rate that potentially is able to match SLR (Kirwan and Megonigal, 2013; Turner et al., 2004). However, this increase also depends on factors such as land subsidence, sediment supply, vegetation productivity, storm frequency and tectonic uplift. Spatial variability in the bed level, channel network and vegetation cover play an important role as well. These either reduce or increase the level of safety against submergence (Bouma et al., 2016; Craft et al., 2009; Crosby et al., 2016; Stralberg et al., 2011; Willemsen et al., 2016). With an accelerated increase in the SLR rate, lower suspended sediment concentrations (as rivers are frequently dammed and groynes reduce alongshore transport upstream) and reductions in the plant productivity, it remains uncertain if the marsh adaptation will be able to keep up with SLR projections (Morris et al., 2002). As such, a better understanding of the processes which govern the development towards a potential equilibrium state and its adaptation under variations in the model parameters is beneficial (Bouma et al., 2016).

Salt marsh ecosystems have been explored extensively with experimental and analytical studies and through numerical models of either a schematized or case specific nature. A range of models have been utilized, which capture in some combination the feedbacks between the biomass contribution, plant growth, tidal dynamics and morphology, to determine the effect of SLR on the bed elevation due to variations in inundation, sediment supply and/or plant productivity due to SLR (Dijkstra, 2008; Temmerman et al., 2007; Van der Wegen et al., 2016; van Loon-Steensma, 2015; Ye, 2012; Zhou et al., 2016). The general conclusions of these studies highlight the importance of the rate of SLR to marsh adaptation. The salt marsh degenerates under high rates of SLR but maintains a stable profile under low or mean SLR rates (Kirwan and Mudd, 2012). Most recently, the patterns in carbon sequestration and accretion data were analysed globally against increases in SLR to compare the actual resilience against modelled quantifications (Nyman et al., 2006). Measured accretion rates over the last century and more so in the last two decades were shown to be lower than the predicted or modelled values which are needed to sufficiently keep pace with SLR (Craft et al., 2009; Crosby et al., 2016). This was concluded for both the conservative RCP 2.6 and the extreme RCP 8.5 climate change scenarios with projected reductions in the marsh cover in excess of 90% for the latter (Craft et al., 2009; Crosby et al., 2016; Morris et al., 2002). However, given more recent estimates for SLR (Horton et al., 2014; Sweet et al., 2017), the RCP 8.5 SLR scenarios may also be seen as conservative.

Therefore, this analysis intends to test the above mentioned behaviour using a schematized process-based numerical modelling approach. The numerical model was developed and validated quantitatively against existing theory, data and laboratory studies. The value of the current study compared to earlier studies is threefold. Firstly, we considered an integrated marsh-mudflat system including the sediment exchange between the mudflat and marsh. Secondly, we explicitly considered wave action as the main driver for sediment re-suspension with the associated tidal sediment dynamics. Finally, we followed a 2D area approach accounting for the spatial dynamics of the marsh-mudflat. Although the focus of this study is on a process understanding of the behaviour of the salt marsh-mudflat system, the schematized model setup was inspired by the conditions found in the Dutch South-Western Delta.

2. Methods

2.1. Bio-geomorphological model methods

Our schematized process-based, numerical modelling approach couples tidal hydrodynamics, wave action, sediment transport and morphodynamics (Delft3D); with vegetation growth and bio-accumulation (via a MATLAB code). Both the Delft3D software and the MATLAB tools utilized in this study are open source (https://oss.deltares.nl/web/delft3d).

2.1.1. Morphodynamic model approach

The Delft3D-FLOW model solves the unsteady shallow water equations in two dimensions (depth-averaged) since preliminary sensitivity runs showed that a 3D approach leads to similar results (Van der Wegen and Roelvink, 2008; Willemsen et al., 2016). Similar to Van der Wegen et al. (2016), sediment erosion and deposition rates are calculated using the Krone-Partheniades formulation for fine (muddy) sediments. Sediment transports are calculated based on the advection-diffusion equation for the long term geomorphological development (decades). The bed level is updated every time step based on spatial gradients in sediment transport. The application of a morphological factor (100) enhanced the bed level development compared to hydrodynamic timescales (Roelvink, 2006). Theoretically, the use of the morphological time factor, which accelerates the bed level variations, can be easily applied to the growth, diffusion and decay processes but is limited for the establishment. However, within our model the bio-geomorphological time scale is significantly larger than the hydrodynamic time scales and therefore any changes wouldn't significantly impact the hydrodynamics (Attema, 2014; Roelvink, 2011).

The 10 m grid resolution and domain applied were determined by the visibility extent of the desired features within the salt marsh-mudflat system, such as the establishment and growth of the vegetation and, the expected channel dimensions (Attema, 2014; Lokhorst, 2016;

Oorschot et al., 2016). Cliff dynamics, at the marsh edge, are not within the scope of this study. Comparisons with a 5 m grid resolution showed minimal variation in the geo-morphological developments along the platform and interface. Application of a cut-cell approach to cover cliff dynamics in our methodology may be the subject of future research.

Wave action was represented by the roller model extension of Delft3D (Hydraulics, 2002) as it is less computationally intensive than other, more sophisticated wave models like SWAN. The roller model predicts short wave groups propagating over a bed including wave dissipation by breaking and bed friction. Although the flow is impacted by vegetation friction, the presence of vegetation does not affect the roller model bed friction in the current model formulation.

2.1.2. Dynamic vegetation model approach

The vegetation growth module applies the population dynamics approach described by Attema (2014), Schwarz et al. (2014) and Temmerman et al. (2005). However, the coupling techniques and the representation of the vegetation across timescales were adapted for the trachytope extension of Delft3D-FLOW capturing both marsh and mudflat. The net growth of the vegetation is represented by the following relation:

Equation (1): Net Vegetation Growth (Monden, 2010; Schwarz et al., 2014; Temmerman et al., 2007)

$$dP = dP_{est} + dP_{growth} + dP_{diffx} + dP_{diffy} - (dP_{inund} + dP_{flow}) \quad (1)$$

Where:**dP** represents the derivative of the total stem density of the salt marsh w.r.t time (year), [stems/m^2].$\mathbf{dP_x}$ represents the derivative of the stem density of the salt marsh w.r.t time, [stems/m^2] where x = the establishment (est), growth, diffusion, inundation (inund.) and shear stress (flow).

Kindly see Appendix D for additional details. The bio-geomorphological model was developed to represent the influence of one vegetation type during the analysis for the *Spartina anglica* species. After every vegetation time-step the marsh model records the change across the grid domain of the height, vegetation density, drag coefficient, bed roughness and the relative coverage of the vegetation in each grid cell.

2.1.3. Offline coupling approach

The trachytope extension of Delft3D defines the location of the vegetation across the domain. After every morphodynamic time step, the output of Delft3D (bed level, shear stresses, water level and flow velocities) is converted to input parameters for the growth model (inundation and shear stresses). Subsequently, after every vegetation time step the adjusted roughness and flow resistance parameters are then compiled in the trachytope input files (Deltares, 2014). The roughness exerted by the vegetation on the flow is determined using the Baptist et al. (2007) relation, where the higher the value the smoother the surface and the smaller the drag force. Afterward, the Delft3D-FLOW model is then restarted with the new spatial layout of the vegetation and the bed level (Fig. 1).

The seasonal and daily variations in the water level, which impact the spatial and temporal establishment of the vegetation, also constrain the acceptable hydrodynamic and morphodynamic time steps. On the other hand, calculating bed level changes and vegetation growth every hydrodynamic time step (1 min) would lead to excessive computation time. Therefore, using a MF of 100, a single hydrodynamic tide represented three months of morphological development. We coupled the vegetation growth model to Delft3D coupled every three months (each single tide) which roughly covered the seasonal dynamics of vegetation growth. This loop continued until an equilibrium bathymetry and vegetation density were attained.

2.2. Model setup

2.2.1. Overview of typical salt marshes in the South Western Delta

2.2.1.1. Domain schematization. The locations that inspired the current study are located in the Dutch South-Western Delta, more specifically the Hellegat Salt Marsh, The Sint Annaland salt marsh and the Land of Saeftinghe salt marsh (Fig. 2). The marshes, all of which were formed naturally and have open environments subject to both waves and tides, were selected randomly to represent the variability of the marshes in the South Western Delta. This variability extended to the size, layout of marsh to mudflat, channel patterns and velocities. Though these three sites were highlighted, results were also compared to marshes along the Western Scheldt where studies with similar approaches were available (Temmerman et al., 2005; Temmerman et al., 2013; van Loon-Steensma, 2015; Winterwerp et al., 2013).

The three case study locations were chosen to determine both the boundary and domain conditions. They provided descriptions for the dimensions of the domain; however the bathymetry and boundary conditions were chosen to be representative of the Hellegat Salt Marsh. With regards to the quantitative validation of the model results, the data available at the time of this study were detailed towards to the Hellegat Salt Marsh. The dimensions for the length and width of model were chosen so as to ensure a balance between the computational time and an apt representation of the interactions between the salt marsh and mudflat. The model domain would first represent a slice of the typical system, with the smallest possible length of 500 m which would not impede the formation of channels. With the exception of the Land of Saeftinghe salt marshes, the typical width was below 1500 m. Therefore the marsh platform for allowable growth was extended 1500 m with a mudflat at the seaward edge extending a further 1000 m (Fig. 3).

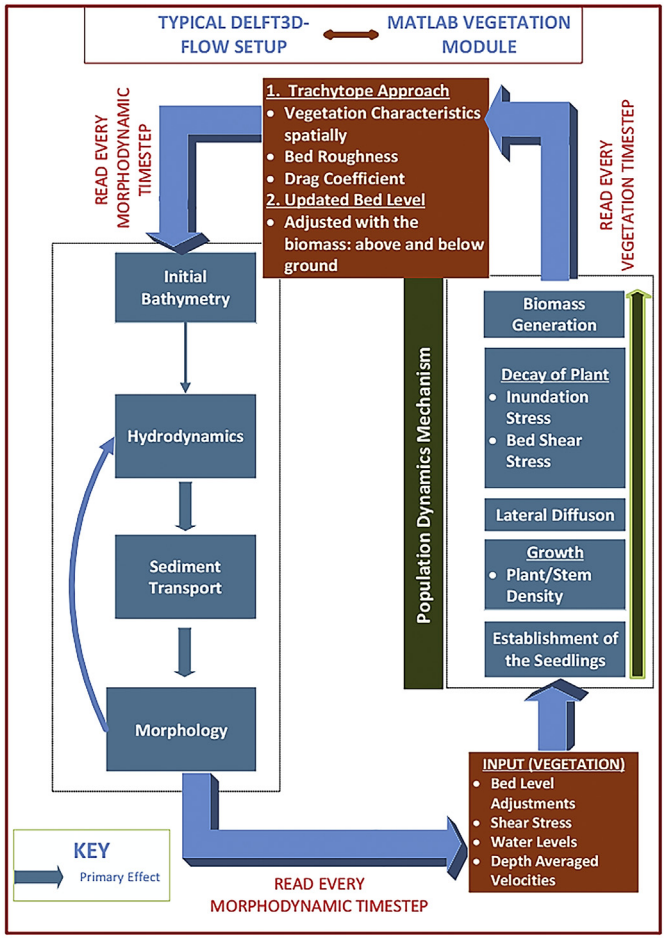

Fig. 1. Detailed explanation of the coupling approach for model setup.

2.2.1.2. Physical setting. The Hellegat salt marsh is situated along a meandering channel and is subject to both the tidal dynamics (semi

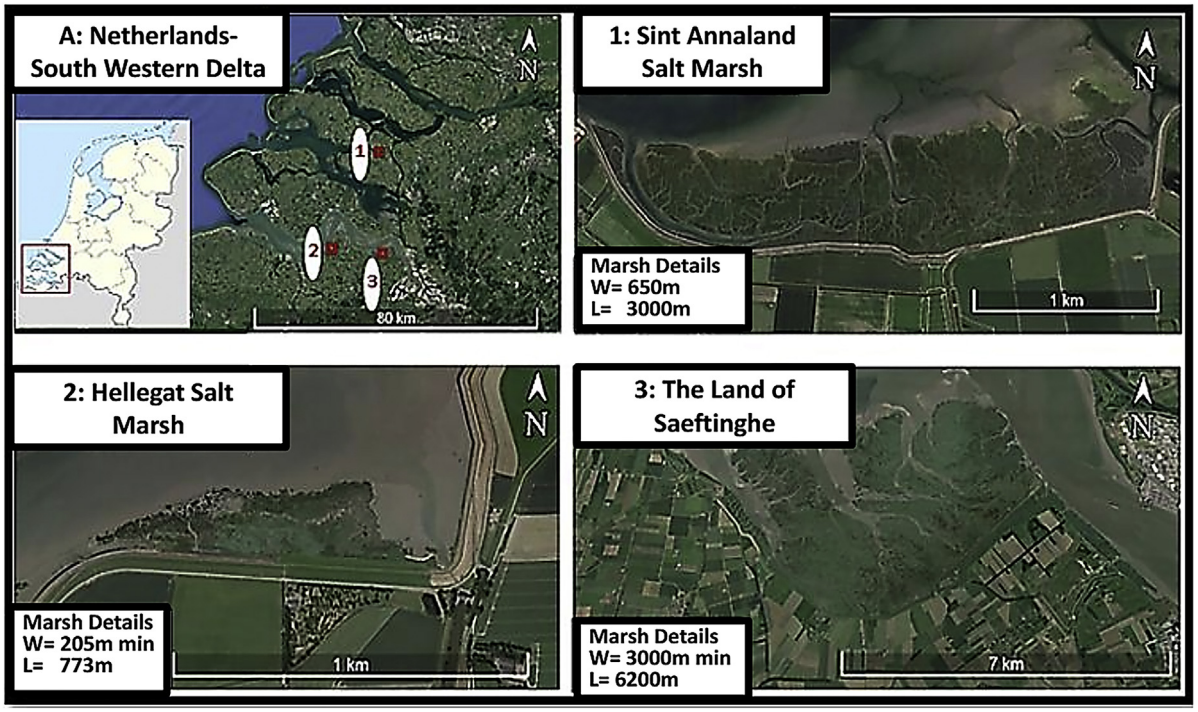

Fig. 2. Three typical salt marsh-mudflat systems within the Dutch South Western Delta used for schematized model setup (Google Earth): (a) Overview of the relative locations of the three marshes; (1) The Sint Annaland Salt Marsh; (2) The Hellegat Salt Marsh; (3) The Land of Saeftinghe. Where W = width of the salt marsh, distance perpendicular to the dyke line and L = the length of the salt marsh, distance parallel to the dyke line.

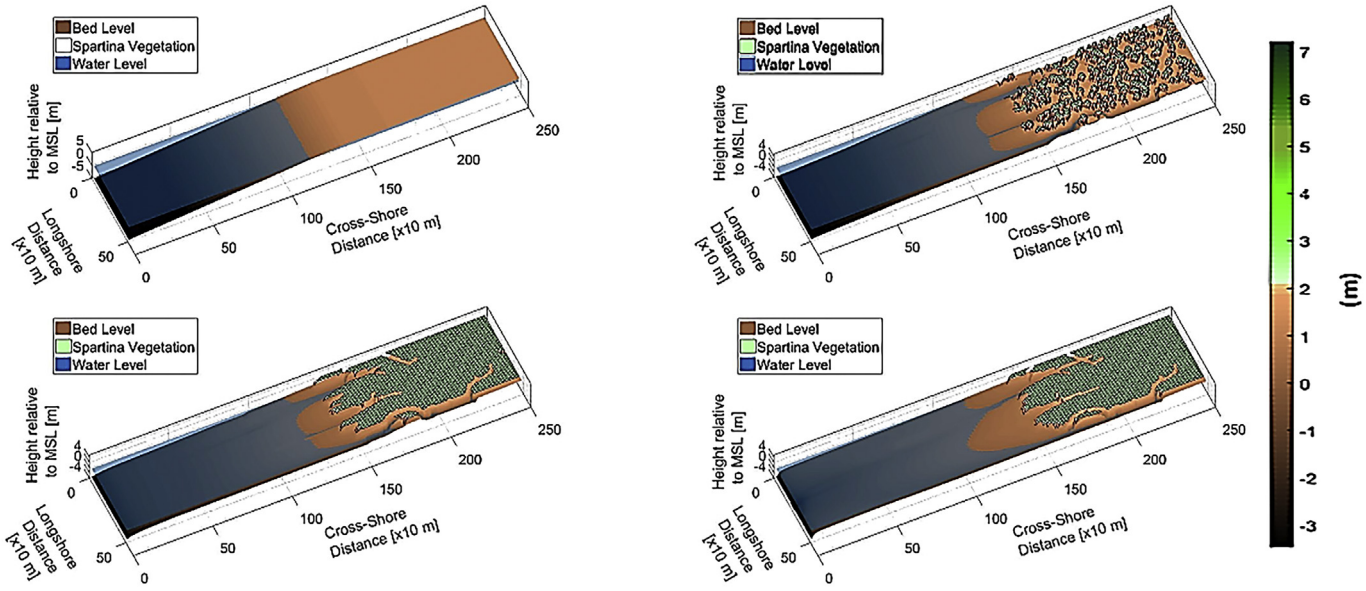

Fig. 3. Evolution of the spatial density of the salt marsh vegetation at different points in time: (a) Initial bed level, and after (b) 20 years, (c) 50 years, (d) 120 years. Colour bar showing the variations in bed elevation and plant height *(1 m)*. (For better interpretation of this figure, the reader is referred to the Web version of this article.)

diurnal tidal regime and a mean tidal range of 3.9 m) and wave action (Vuik et al., 2016). This channel has suffered extensive erosion and is currently reinforced with dykes to protect the hinterland areas. During spring tides, the mean tidal range increases and varies from 4.49 m to 5.93 m. Over the last century, the mean water level has risen by approximately 3 mm at the mouth of the Western Scheldt and 15 mm in the inner section of the estuary (Temmerman et al., 2005). There is a clear reduction in the magnitude of the waves which propagate from the North Sea and dissipate their energy over the smaller depths. During extreme storm events, the wave heights recorded in the Western Scheldt estuary have maximum values ranging from 2 m to 3 m (Li et al., 2014; Sistermans and Nieuwenhuis, 2004). However, average wave heights near the marsh are about 0.7 m and slowly decrease as the waves propagate over the vegetated marsh which has a maximum depth of 1.9 m above the marsh surface (Vuik et al., 2016).

The sediment compositions of the estuary consist of fine sediments with sizes ranging from 24 μm to 56 μm in the channels, mudflats and deeper parts of the shoals, while along the vegetated salt marsh sections the size is approximately 88 μm. However, despite the classification as a cohesive sediment area, it should be noted that there is a bit of fine sand

Table 1
Properties for the model set-up for salt marshes (Hu et al., 2009; Temmerman et al., 2007).

Parameters	Values (S.A)	Unit	Reference/Source
Seed, Chance of Establishment, Seed	0.01	[yr $^{-1}$]	Temmerman et al. (2007)
Initial Plant Density, P_0	200	[stems m^{-2}]	Attema (2014)
Intrinsic Growth Rate, r	1	[yr $^{-1}$]	Temmerman et al. (2007)
Max. Carrying Capacity for the plant density, K	1200	[stems m^{-2}]	Attema (2014)
Plant Diffusion Coefficient, D	0.2	[m^{-2} yr^{-1}]	Temmerman et al. (2007)
Plant Erosion Coefficient due to Bed Shear Stress, C_τ	30	[stems m^{-2} per Nm^{-2}]	Temmerman et al. (2007) D3D Output interval: 10 min
Critical Bed Shear Stress for Plant Erosion, τ_{cr}	0.26	[Nm^{-2}]	Temmerman et al. (2007)
Plant Erosion Coefficient due to Inundation Stress, C_{inund}	3000	[stems m^{-2} per m]	Temmerman et al. (2007)
Critical Inundation Height at High Tide, H_{crp}	1.4	[m]	Temmerman et al. (2007)

Where: S.A: *Spartina anglica*.

in the system which results in maximum sizes of 119 μm in the densely vegetated areas (Rahman, 2015). The coarser sediments were not considered due to the intended schematization of a developing marsh. The Hellegat salt marsh has geomorphological development characteristic of an old, high marsh with a relatively flat platform, 1:40 slope, dissected by a developed network of channels or tidal creeks (Temmerman et al., 2004). The average marsh elevation is 1.1 m + NAP (Dutch ordinance level, which is close to local mean sea level) (Bouma et al., 2016). *Spartina anglica* dominates the marsh vegetation with an average number of stems/m^2 of 1200 and an average stem thickness of 3 mm (Vuik et al., 2016). Beyond the edge of the salt marsh platform, there exists a bare tidal mudflat which eventually deepens as the centre of the channel approaches. It is important to note that at the time of the research, information regarding the soil sediment composition and the effects of wind waves were not available.

2.2.2. Detailed schematization & model parameters

The model setup describes a 2DH section of a salt marsh-mudflat system, 2500 m cross –shore by 500 m longshore with grid cells of a 10 m grid resolution. The grid cell size is apt as channel widths within the Western Scheldt are often of a magnitude of 10 m. The bed increases from -5 m at the seaward boundary (only open boundary) to 1 m at the edge of the initial mudflat platform over a cross shore distance of 1500 m. The platform then further extends another 1000 m to the landward boundary. Along the platform random perturbations of +1 cm were added to the bed level to stimulate pattern development. A uniform Chézy roughness value of $65 m^{1/2}/s$ was used to represent a smooth bed of cohesive sediment without vegetation. The model was forced with a harmonic water level boundary at the seaward edge having a single 12 h period tide of 2 m. The length of the tidal cycle extended 21 h with a hydrodynamic spin up time of 540 min, and a 12 h period including geomorphological development. A constant wave climate was imposed consisting of waves with 0.5 m significant wave height (Vuik et al., 2016; Vuik et al., 2016), a 2 s peak period and entering the domain perpendicularly.

A uniform suspended sediment concentration (SSC) of 0.025 kg/m^3 was defined at the seaward boundary with a Thatcher-Harleman time lag of 120 min. This time lag describes the period of gradual SSC change at the seaward boundary at the turning of the tide and prevents sudden variations in the suspended sediment concentrations and associated numerical instabilities. The model assumes zero gradients alongshore. Areas with a shear stresses in excess of a critical shear stress of 0.5N/m^2 will be eroded. Deposition occurs at a rate of the product of the fall velocity (w = 0.5 mm/s) and the SSC. For further detail, see Appendix A for a compilation of the model parameters.

Within the context of this research, equilibrium will depend on both the vegetation density and the geomorphological developments. For the geomorphology aspect, equilibrium may refer to a profile which has a dynamic nature over longer timescales but remains static or stable vertically or horizontally over shorter timescales. The lateral retreat or expansion of the leading edge of the marsh is characteristic of the shift horizontally, while the vertical movement refers to the increase or decrease of the bed elevation. Salt marshes attain an equilibrium density after 20–30 years during favourable site specific conditions (Attema, 2014; Schwarz et al., 2014), with the geomorphological development attaining equilibrium on a decadal scale. Therefore, the model extended for 120 years of vegetation growth (see Table 1 for parameters) to capture a profile in equilibrium.

The SLR was imposed with both a linear and exponential increase. To achieve this the mean sea level (MSL) was raised at the end of each year by a value prescribed by a linear or exponential function for the IPCC RCP 8.5 climate scenario. The IPCC was chosen over the National Oceanic and Atmospheric Administration (NOAA) due to its global applicability and coverage. After an equilibrium mudflat profile was generated over the 120 years, the SLR scenarios were imposed over 100 years. The MSL increases by 1.137 m under the high approximation and 0.6 m and 0.8 m for the low and mean approximations respectively. The contribution of the biomass (above and below ground) is examined via sensitivity runs where the range varies from a conservative contribution of 1 mm/year to 3 mm/year (Craft et al., 2009; Crosby et al., 2016; Morris et al., 2002; Temmerman et al., 2013; van Maanen et al., 2015). Scenarios also included variations in the wave height, SSC, sediment properties and yearly accretion balances within the marsh (6 mm/year and 9 mm/year) (Crosby et al., 2016).

3. Bio-geomorphological development and model validation

3.1. Development to equilibrium

During the initial years the geomorphological development of the salt marsh-mudflat system was found to lead the salt marsh growth, as plant establishment is limited by inundation and erosion stresses (Fig. 3). Initially, the vegetation establishes in patches on the platform, resulting in the formation of channels due to flow concentrations around these patches. As the channels incise the platform further, deposition of sediment along the banks of the channels form characteristic levees (See Appendix B: Video 2 **for the animation of the Salt Marsh-Mudflat base model: Supplemental Materials**). When the vegetation reached its maximum stem density after 35–40 years, the channel patterns are stabilized by the vegetation and they form the main drainage area for the intertidal vegetated zone. Geomorphological development is then limited to the heightening of the marsh with a slow progradation of the marsh edge (Appendix B). The channel flow is asymmetric with a short, high velocity flood period and a long low velocity ebb period. The magnitude of the velocities within the vegetation were notably lower than the channels but maintained the characteristic surges during flood and ebb.

Supplementary video related to this article can be found at https://doi.org/10.1016/j.envsoft.2018.08.004.

Even after 120 years, the marsh edge continues to prograde due to the supply of sediments from the seaward boundary. Shear stresses near

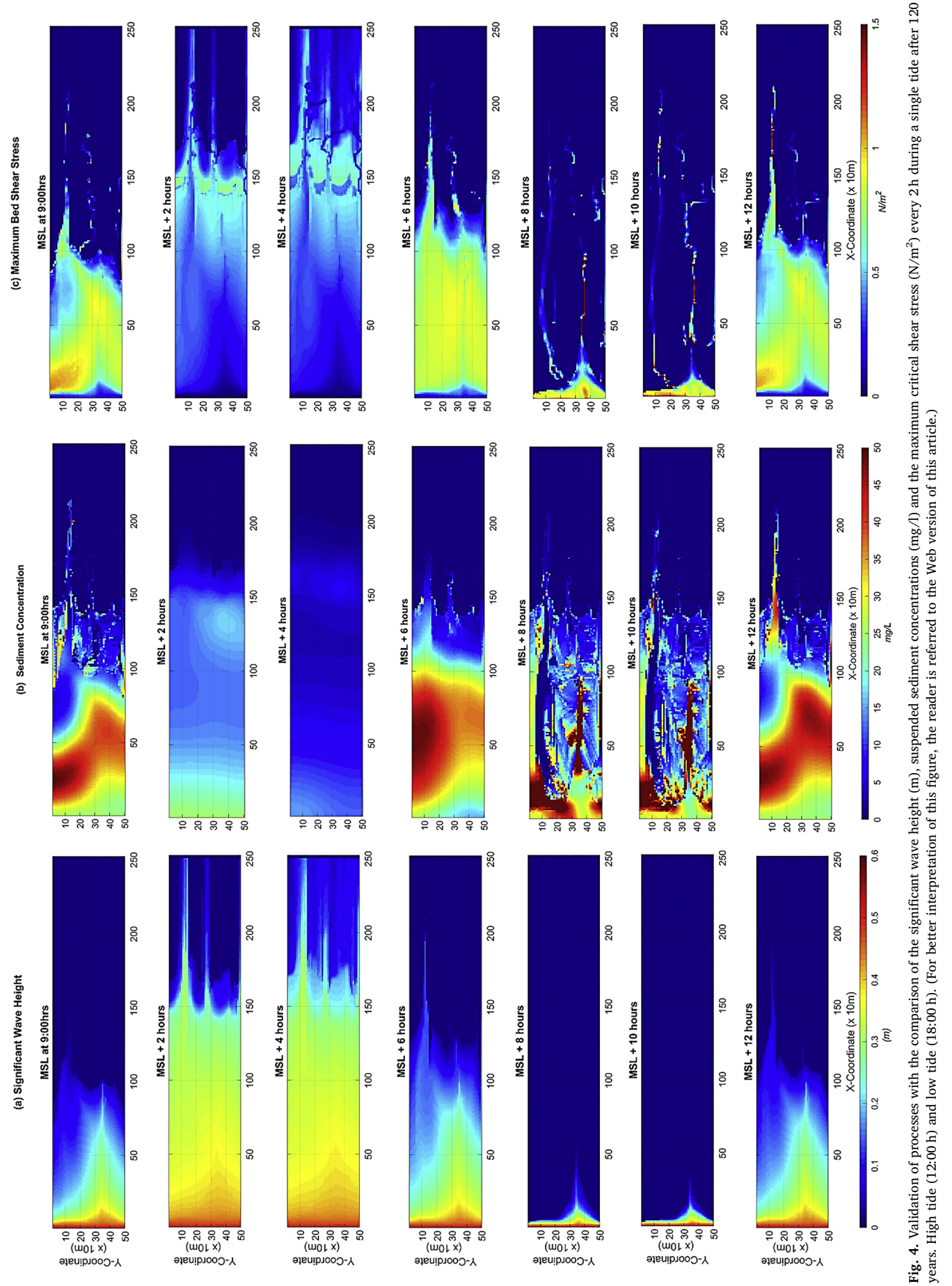

Fig. 4. Validation of processes with the comparison of the significant wave height (m), suspended sediment concentrations (mg/l) and the maximum critical shear stress (N/m^2) every 2 h during a single tide after 120 years. High tide (12:00 h) and low tide (18:00 h). (For better interpretation of this figure, the reader is referred to the Web version of this article.)

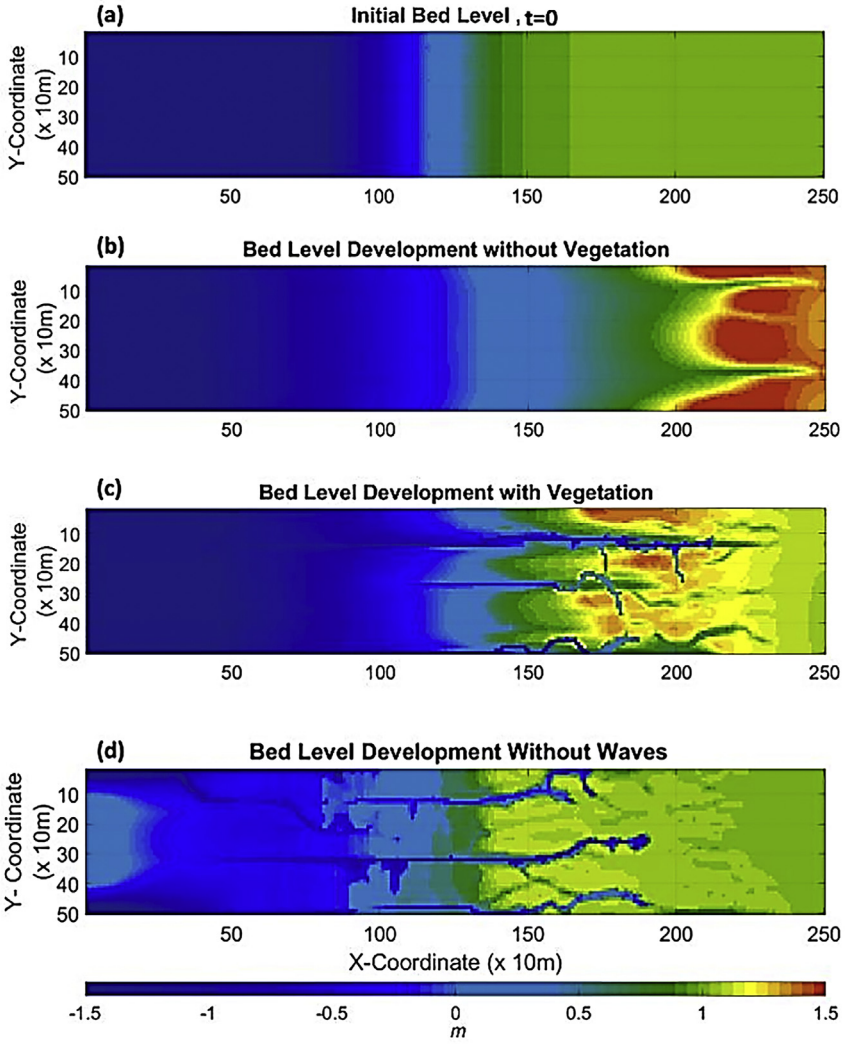

Fig. 5. Comparison of the Initial Bathymetry and the Bed Level (a) initial profile, (b) without vegetation, (c) vegetation + waves + tides, (d) Without waves after 120 years. (For better interpretation of this figure, the reader is referred to the Web version of this article.)

the marsh edge and in the incising channels continue to exceed the critical shear stress for erosion, 0.5 N/m^2 (Fig. 4 and Fig. 5). The main reason for this being the dissipation of the wave energy. For a similar, yet 1D, study Van der Wegen et al. (2017) showed that geomorphological equilibrium is eventually reached by an evolving mudflat despite the fact that the critical erosion shear stress is continuously exceeded during the tide. Although, wave action leads to high shear stresses and related high sediment concentrations, the tide residual sediment transport becomes negligible so that there is no net geo-morphodynamic development. Net sediment deposition occurs mainly behind the marsh edge and around the channels in levee formation deposits (Fig. 6 and Appendix C). After the 120 years the marsh profile shows minimal variation. Equilibrium is not reached in the strict sense since the marsh edge continues to prograde at a slow rate. Nevertheless, the system was considered to be stable to allow further sensitivity and SLR scenario analysis. **(See video animation in** Appendix B**).**

3.2. Impact of vegetation & waves on the morphology

Without vegetation, the channel (braiding) patterns are replaced by straight channels which incise the platform further while allowing for the distribution of the sediment across the mudflat (Figs. 5 and 6). The channels are able to incise the platform further because of the low roughness in the absence of the vegetation. The level of the platform, despite being narrower than the vegetated case, becomes higher as sediments are easily transported landward. When the waves are excluded, the vegetated platform is wider as the reduced re-suspension supports the progradation. However, the transport of the suspended sediment into the marsh, toward the landward sections, is significantly lowered. Waves lead to higher matured marshlands. The presence of the vegetation increased the flow velocities within the channel while resulting in a significant decline of the velocities on the shoals.

Larger height differences between the muddy marsh and the mudflat enhanced the erosion rate, steepening the transition, especially in the presence of waves (Figs. 6 and 7(a)). This observation is similar to that of Bouma et al. (2016) and Bouma et al. (2005). Fig. 7(d) shows that the magnitude of the wave forcing will contribute towards the development of steep transitions at the marsh edge.

3.3. Sensitivity analysis: process understanding

Here, we have summarized the results for high-impact parameters which affect vegetation density and bed level (Figs. 7 and 8). The findings provide possibilities for realistic adaptations in restoration and protection measures. NB: For this system, marsh platforms below 0.7 m above the mean water level did not support the establishment of the vegetation.

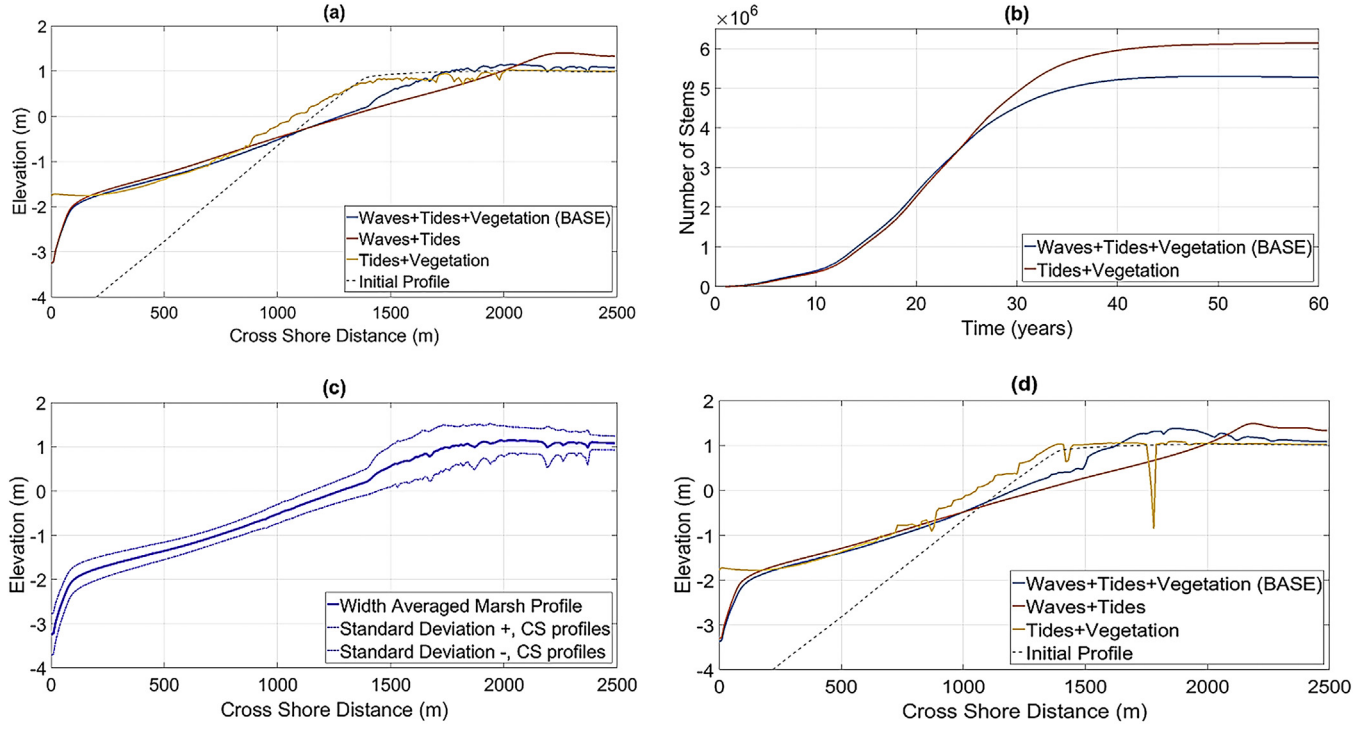

Fig. 6. Evolution of the (a) width averaged bed level and (b) growth of the stems for variations of physical processes, (c) spatial distribution of the bed level for the base run and (d) bed level along specific cross section.

3.3.1. Wave height

From the analysis of the base model, waves have been identified as the main driver for the lateral retreat (Appendix B, Figs. 5 and 6) of the marsh platform. Waves suspend sediments from the mudflat and these sediments are transported landward during flood. Sediments deposited landward are subject to limited shear stresses, due to the trapping capacity of the marsh, so that ebb currents transport less sediment seaward during ebb. This resulted in the heightening of the platform level as sediments filled the accommodation space. Therefore, the variation in the wave height provides an understanding of the system behaviour under varying wave climates. Overall, Fig. 7 (d) shows that larger waves produce steeper marsh edge transitions with a retreating edge. Conversely, lower waves allow for larger sections of high marsh lands on which mature and stable plant species reside. Compared to purely tidal environments, waves are seen to create higher platform levels. When the wave height is lowered, the geomorphological developments resemble that of a purely tidal environment. In alternative wave climates, this can be used as a tool in promoting growth within restoration strategies. Fig. 8 (d) also reveals that an increase of the wave height lowers the vegetation coverage, where the doubling of the wave height results in an approximate reduction of 1×10^6 stems/year.

3.3.2. Roughness, tidal amplitude and platform bed level

A higher roughness (lower Chézy value) leads to a concentration of flows generating narrower and deeper channels which prograde into the marsh area further. Additionally, a higher roughness enhances the erosion of the mudflat and platform due to enhanced sediment suspension resulting in a retreating marsh edge and heightened platform (Fig. 7 (i)). Within the morphological model, the constant Chézy value affects flow and sediment transport (bare areas only), and wave attenuation. The roughness generated by the vegetation affects only the flow and sediment transport in marsh areas.

As the tidal amplitude is lowered with a constant platform height, the degree to which the platform is flooded reduces. Therefore, the mudflat is eroded because the waves dissipate all of their energy on the mudflat. At the marsh edge, continual wave dissipation results in the deepening of the mudflat level and the formation of steep transitions. When the tidal amplitude equals or exceeds the magnitude of the marsh level, the wave dissipation is limited within the area of the mean water high level and gentler transitions are formed at the marsh edge.

Regarding the evolution of the stem growth, lower tidal amplitudes and by extension lower inundation stresses allow for higher stem densities within the domain (Fig. 8). The platform level variations show a greater affinity for the distribution of sediment along the transition area and mudflat whereas the variations in the amplitude allow for sediment to be deposited along both the marsh platform and also at the transition area (See Appendix C: Figure C2).

3.3.3. Sediment characteristics

With the combination of both waves and tides the typical range for the shear stress lies between 0.3 and 0.5 N/m^2. This range is in line with validated model studies including wave action and tidal forces (Borsje et al., 2011; Cheon and Suh, 2016; MacVean and Lacy, 2014; Townend et al., 2011; Van der Wegen et al., 2016). Results (Fig. 7(c)) reveal that lower critical shear stress values lead to an eroding mudflat and a landward transport of sediments building up the marsh platform. Therefore, restoration efforts which, in practice, simulate sufficient stirring of the sediment offshore will allow for increased deposition within the marsh. Lower fall velocities lead to a similar behaviour (Fig. 7(h)). However, though the marsh is elevated, the width is reduced due to the lateral retreat of the platform. The stem density is reduced with lower critical shear stress and fall velocity values (Fig. 8(c)). The runs with a lower critical shear stress produce straight-lined channel patterns with increased mortality rates. However, generally the modelled channel formation patterns and channel and marsh velocities are overestimated compared to the values found in literature (Kirwan and Megonigal, 2013; Maan et al., 2015; Temmerman et al., 2007; Temmerman et al., 2010). This may be attributed to the use of the roller model to represent the wave energy, where due to the lack of diffraction considered along the one directional plane of movement, the shear stresses are often in excess of 0.5N/m^2 especially during the flood tide. The marsh platform seems not heavily affected by the boundary

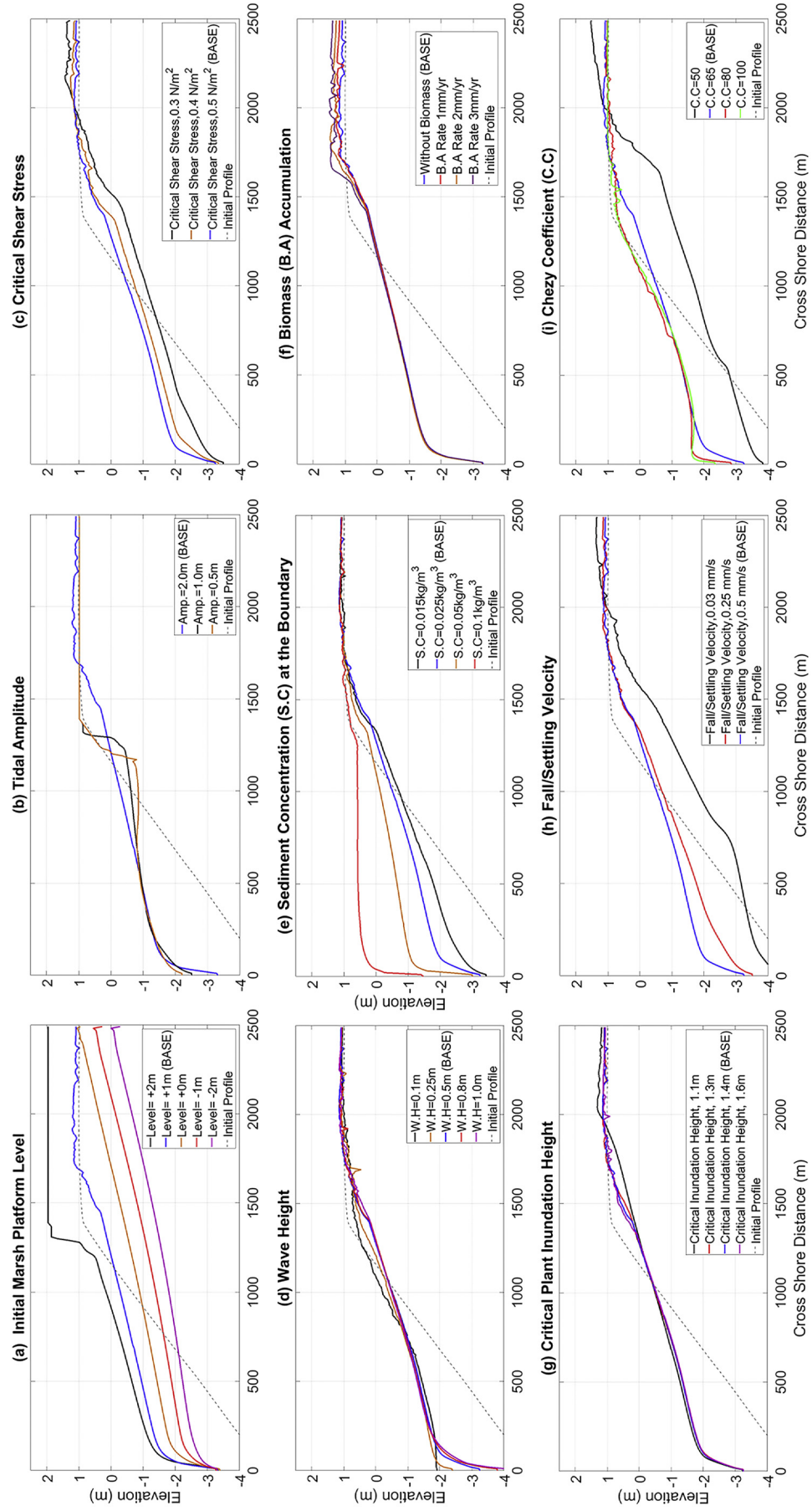

Fig. 7. Sensitivity results panel summarizing the effect of variations in the key model parameters on the geomorphological development.

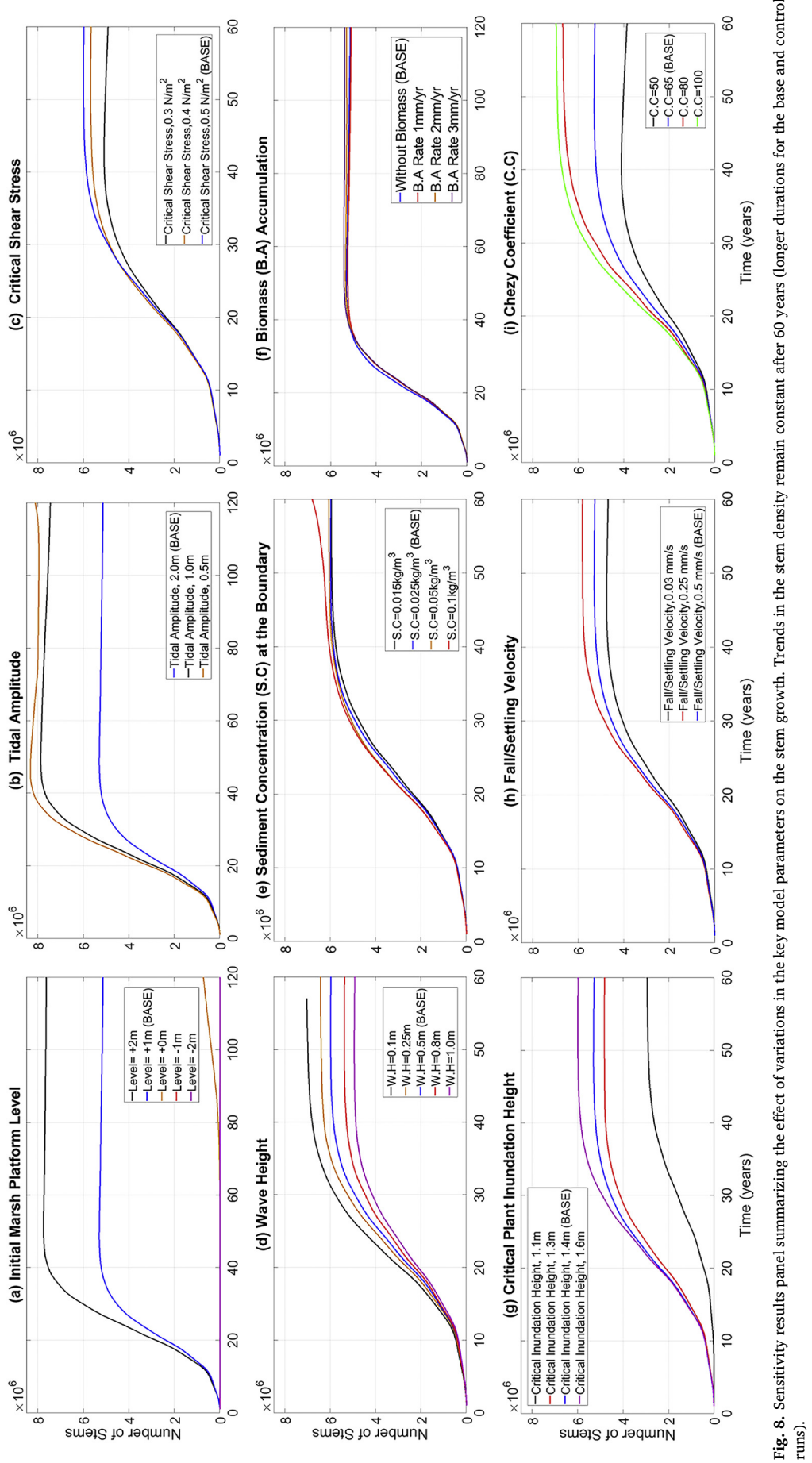

Fig. 8. Sensitivity results panel summarizing the effect of variations in the key model parameters on the stem growth. Trends in the stem density remain constant after 60 years (longer durations for the base and control runs).

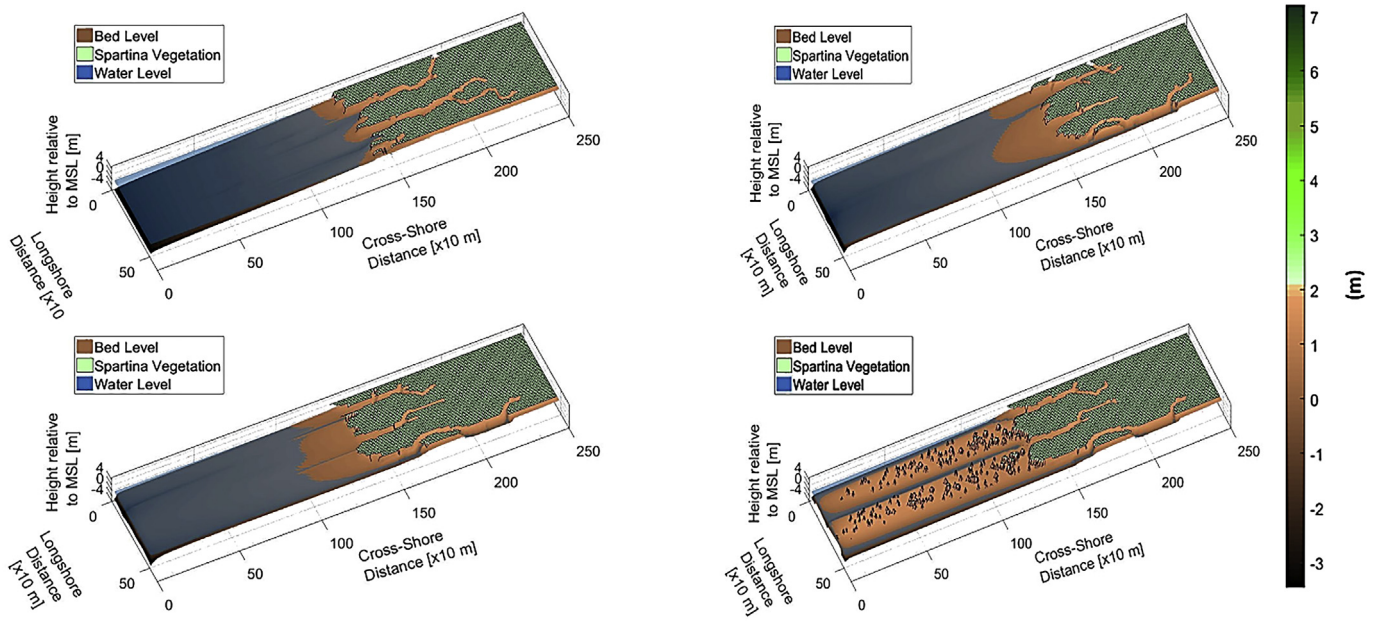

Fig. 9. Variation of the stem density and the bed level for a gradual increase in the sediment concentration from (a) 0.015 kg/m^3, (b) 0.025 kg/m^3, (c) 0.05 kg/m^3 and (d) 0.1 kg/m^3. (For better interpretation of this figure, the reader is referred to the Web version of this article.)

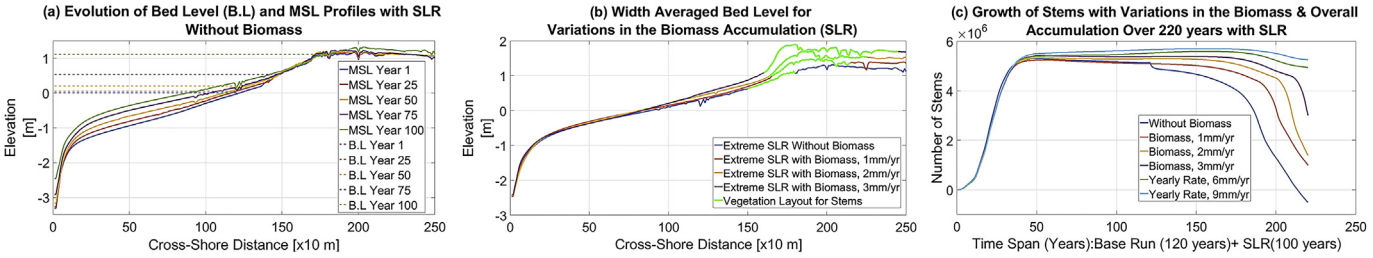

Fig. 10. (a) Evolution of the width averaged bed level under SLR without biomass, Comparison of (b) the width averaged bed levels for biomass variations and the (c) stem density for the scenarios with biomass and yearly accretion rate under the high approximation for SLR. The green section of the width averaged profile highlights the location of the vegetation. (For interpretation of the references to colour in this figure legend, the reader is referred to the Web version of this article.)

sediment concentrations (Fig. 7(e)), but the mudflat is higher for a larger SSC at the boundary. During flood the SSC levels are lower than the SSC imposed at the boundary (25 mg/l). In ebb flow, higher SSC are observed in the channels along the mudflat with minimal values in the channels within the salt marsh. As such, sediments are deposited readily along the mudflat where fall velocities are optimum. Higher SSC values result in a filling of the accommodation space allowing for the progradation of the marsh (Fig. 9).

3.3.4. Plant growth characteristics and biomass

Most morphological variation was seen in the critical inundation height runs (Fig. 7 (g)), followed by the plant height. The less resilient the plant species is to inundation, the lower the stem density. The lower vegetation coverage, then allows for greater deposition along the marsh as higher sediment loads are transported to the marsh (Fig. 7).

As the height of the vegetation increases, the lower the flow velocities and the magnitude of channel incisions in the marsh platform. This adds to the protection offered by the vegetation to the marsh-mudflat edge during ebb flow as the reduced velocities will result in smaller magnitudes of erosion due to flow. With lower plant heights, there is increased erosion of the marsh edge as the transition steepens.

Once the maximum stem density coverage is reached, this results in a more pronounced formation of channels within the marsh platform. Channels in the marsh area become narrower limiting the transport of sediment into the marsh. Relative increases in the marsh platform are notably lower. With the decrease in elevation at the marsh edge, there is an overall regression of the marsh edge with continued dynamics at the boundary after 120 years. Model results show not only the heightening of the marsh platform but the gradual progradation of the marsh edge are observed as the accommodation space is filled for larger bio-accumulation rates (Fig. 7 (f)).

The validation of the plant growth and decay characteristics were carried out quantitatively based on comparisons with Attema (2014) and Monden (2010).

3.4. SLR scenarios

In all three SLR scenarios the landward low-lying areas drown, leaving zones of elevated vegetated land masses disconnected from the shore (Figs. 10 and 11) (See Appendix B: Video 1 for the animation of the Salt Marsh-Mudflat base model: Supplemental Materials). The landward sections of the marsh are relatively low due to the levee formation closer to the marsh edge. The profiles reveal that under the SLR scenarios the bed level increases, but at a rate that is insufficient to match the rate of SLR as shown by the stem density plots in Figs. 10 and 11. As such, there is a loss of the intertidal wetland over time, initially quite gradual, but then increases after 50 years of SLR for the model without biomass contributions (Fig. 10 (b)). This translates to a landward shift of the salt marshes to survive, where space is available. The SLR results in increased water depths which allow waves to propagate further into the salt marsh. The larger tidal prism increases the flow velocities thereby enhancing seaward erosion and landward deposition.

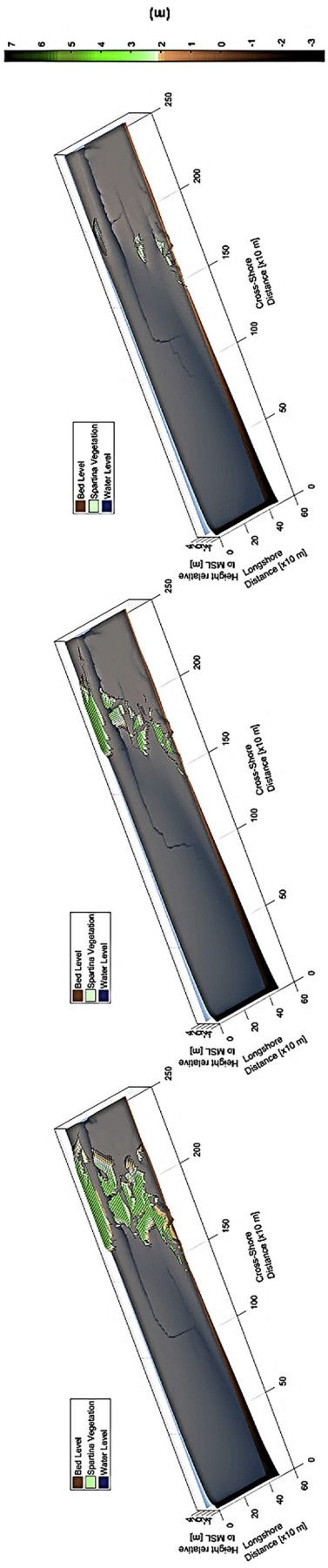

Fig. 11. Evolution of the Salt marsh- Mudflat System in response to Sea Level Rise after 100 years, (a) With the low approximation for SLR, (b) With the mean approximation for SLR, (c) With the high approximation for SLR. (For better interpretation of the figure, the reader is referred to the Web version of this article.)

Sediment is being transported from the mudflat unto the marsh which heightens, but drowns due to insufficient volumes. Under the exponential increase in the sea level, there is a threshold below which the salt marshes can survive and this extends some 40–50 years for all scenarios (Fig. 10 (b)). However, beyond this period, the high water level begins to drown areas that once formed the upper intertidal areas. The vegetation mortality now switches to one dominated by inundation stresses. Overall the salt marsh system, without interventions, will not survive the long term impacts of SLR.

A comparison was carried out between the exponential and linear increases in the mean water level. The exponential scenario did reflect an extended period for which the salt marshes were able to increase the bed level at a rate that exceeded the SLR but the linear scenario only extended approximately 10 years of SLR. However, after 100 years of SLR, the vegetation cover for both systems was the same. It should be noted that this model was developed for sediment rich systems and not sediment poor systems such as in the East of the USA.

4. Discussion

Our schematized 2D depth averaged model satisfactorily describes the interaction between the waves, tides, sediment transport, morphodynamics in Delft3D-FLOW, and the bio-accumulation and plant growth dynamics of the Spartina anglica in MATLAB. The research aimed to increase the process understanding of the salt marsh system and also allow for applications toward resilience measures under SLR. Inspired by the Dutch south western Delta, the bio-geomorphological model reproduced a realistic salt marsh-mudflat system in near equilibrium after a century while reaching a maximum stem density after 40 years. The interaction between the mudflat and marsh area provides key details on the triggers for the geomorphological developments within the marsh-mudflat system. Wave action was found to be the primary trigger for the sediment supply towards the salt marsh with the formation of steep marsh edge transitions. As the waves enter the domain, most of the energy is lost through wave breaking and dissipation along the mudflat. Sediment is continuously stirred and transported to the marsh area. Sediment deposits in the marsh in levee-type patterns close to the channel edges and platform edge. Once the vegetation establishes and grows on the platform, the roughness increases favouring more deposition on the platform. More landward areas face less deposition.

As the elevation of the marsh platform increases, the wave energy becomes concentrated around the mean water level. This results in a dynamic oscillatory flow pattern which erodes the sediment and transports it along the edge of the marsh. This observation is similar to that of Bouma et al. (2016) and Bouma et al. (2005), who suggested that larger height differences between the muddy marsh and the mudflat enhance the erosion rate especially in the presence of waves. This sediment is later transported landward following the channels. As the wave height increases, there is greater transport of sediment towards the platform with steeper transitions between the marsh and the mudflat. Steeper transitions are as a result of the larger magnitude of the oscillatory wave forces. This may be critical for restoration strategies which attempt to promote growth in alternative wave climates. Additionally, when compared with a tidally dominant system, coastal areas exposed to waves have higher marsh platforms.

A system's resilience to SLR will depend on its ability to increase the bed level at a rate that exceeds the SLR. This rate is dependent on the inundation depth at high tide, the external sediment supply and the organic deposition potential. We found that the salt marsh-mudflat system drowns under all imposed SLR scenarios to varying degrees with variations in the sediment supply and biomass. However, the bio-accumulation rate is the most critical parameter affecting the resilience under SLR. High bio-accumulation rates even lead to marsh survival including the heightening and gradual progradation of the marsh (Fig. 12). Results show that the bio-accumulation rate has a greater impact on bed level increases under SLR, once the vegetation density is

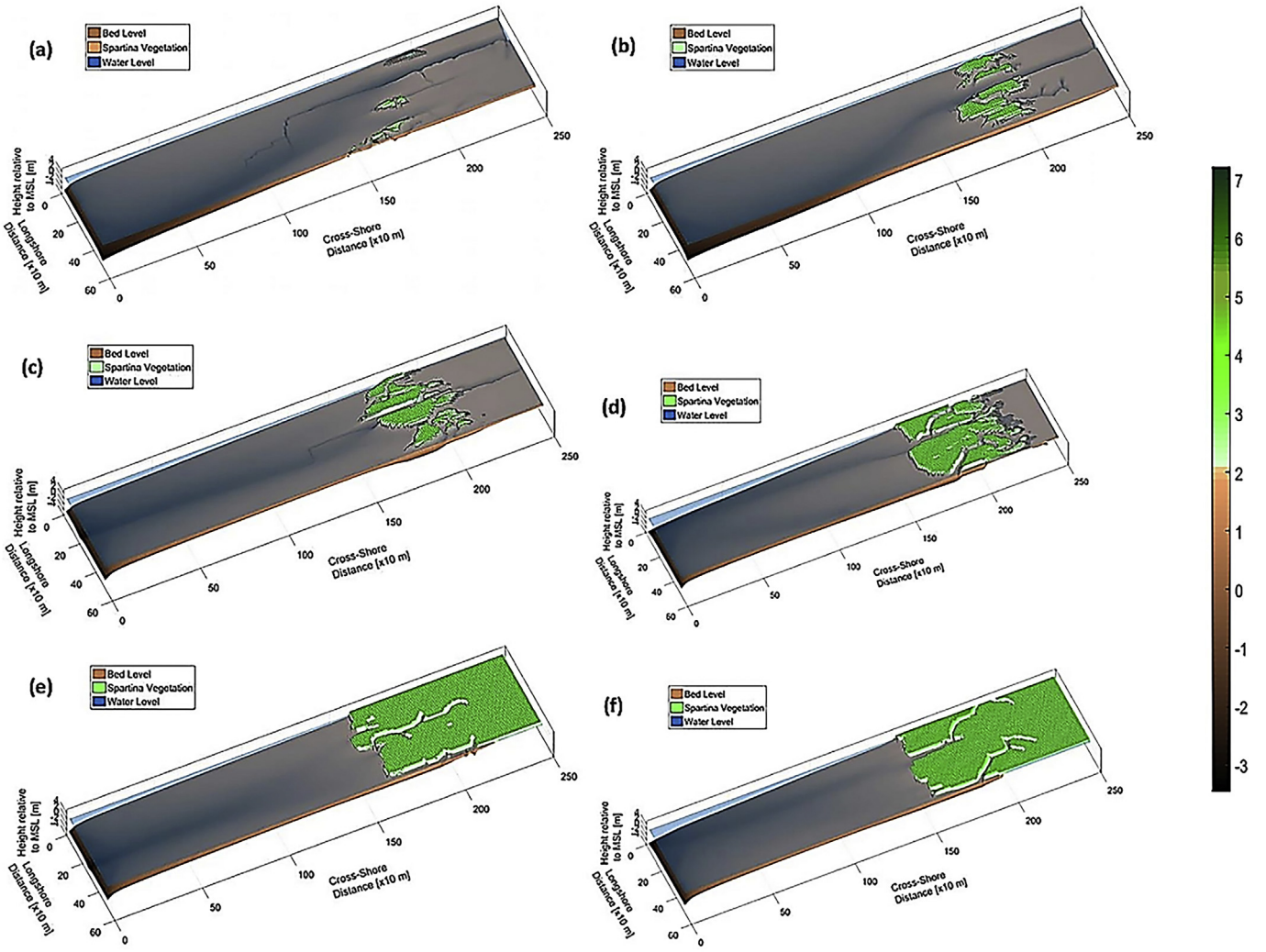

Fig. 12. Comparison of the remaining plant density of the salt marsh under the 1.137 m increase in the mean water level for SLR with biomass scenarios (a) no biomass, (b) the 1 mm/yr, (c) 2 mm/yr, (d) 3 mm/yr, and with yearly accretion rates of (e) 6 mm/yr, (f) 9 mm/yr after 100 years of sea level rise.(For better interpretation of the figure, the reader is referred to the Web version of this article.)

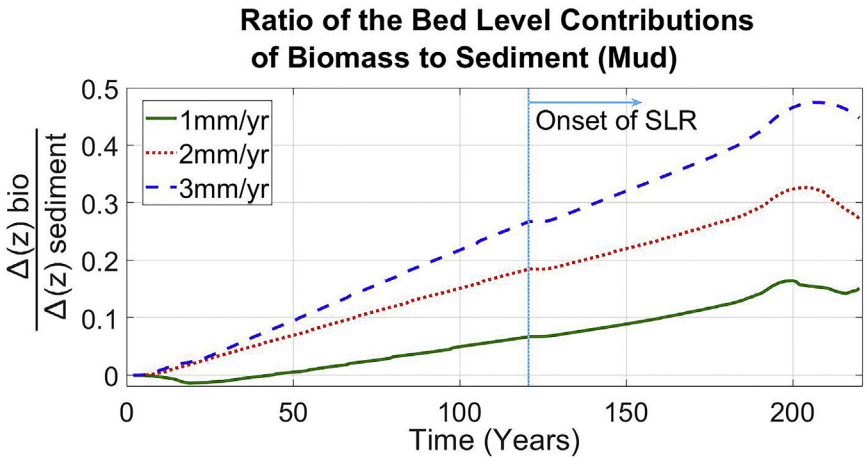

Fig. 13. Relative Contributions of the biomass and sediment (mud) to the increases in the overall bed elevation given by the ratio over 220 years inclusive of 100 years SLR. Where Δ(z)bio and Δ(z)sediment represents the change in the elevation of the bed level attributed to the biomass and mud respectively. Lower rates show a greater dependence on the natural sediment supply.

maintained. Biomass rates (1–3 mm/yr) contribute substantially towards the overall bed level increases when compared to the sediment supply (Fig. 13). However, in Hellegat salt marsh the biomass production is not sufficient to ensure survival under SLR. Production rates in excess of 3 mm/yr are unrealistic as the marsh has an existing belowground biomass capacity of 1.4–4.7 kg/m^2 (Rahman, 2015). As such, this must be supplemented by increases in the external sediment supply to achieve higher yearly accretion rates. Systems with an accretion balance exceeding 5 mm/yr were found resilient while the marsh platform expands for values up to 9 mm/yr. Moreover, high

accretion balances that consider the sediment budget: external (rivers, offshore & artificial supply) and internal (biomass storage and production), are more effective in reducing vulnerability under SLR. Our modelling approach allows for a closer analysis of the spatial dynamics of drowning (Thorne et al., 2014). Especially, the levee type patterns evolving close to the channel and marsh edges that have a significant impact on the response of the system under SLR. These levee areas are the last to drown under SLR scenarios.

Overall, the inclusion of the wave dynamics proved critical for the geo-morphological developments of the marsh-mudflat system and improved quantifications for resilience to SLR. Further works should however explore the dynamics of the sediment budget for specific locations.

5. Conclusion

Our bio-geomorphological modelling approach was able to reproduce a mudflat-marsh system in equilibrium after 120 years. The process-based methodology allowed for a thorough sensitivity analysis of the model parameter space including hydrodynamic forcing, sediment characteristics and vegetation dynamics with the belowground biomass accumulation. Our findings were quantitatively validated primarily against the findings of relevant modelling studies. The model produced realistic channel formations with characteristic flood and ebb hydrodynamics. Wave action was shown to be a key process as it suspends sediments on the mudflat and transports them to the marsh platform during flood. This resulted in the heightening of the marsh platform and the formation of steep marsh-mudflat transitions. Higher wave heights produce narrower and more elevated marshlands. Our area model showed the evolution of levee type deposition patterns along the channels. The critical shear stress, settling velocity, critical plant inundation height and tidal variations are key model parameters in the bio-geomorphological development.

Imposing 100 years of SLR scenarios on the equilibrium profile allowed us to analyse key factors impacting the resilience of the marsh-mudflat system to SLR. Despite the net import of sediments and biomass productivity of the system all SLR scenarios eventually led to the partial or complete drowning of the marsh-mudflat system. The channel networks expanded landward and incised the marsh platform. The vegetated levee-type patterns were the last features to survive. Exponential increases in SLR showed extended periods in which the salt marshes were able to increase the bed level at a rate that exceeded the SLR but the linear scenarios did not. Imposing higher accretion rates may allow the salt marsh survive SLR scenarios. Another key to marsh survival under SLR will stem from increasing the overall sediment supply allowing for higher yearly accumulation rates.

Model approaches with ecological components enhance the process understanding and reinforce innovative solutions in the restoration and protection of these valued intertidal vegetation species. Future research may utilize process-based approaches to evaluate engineering solutions for protection and restoration strategies and study the dynamics of other vegetation types like mangroves with applications to case specific areas.

Software and/or data availability

We applied a process based numerical modelling approach which coupled offline Delft 3D-FLOW and MATLAB. Both the Delft3D software and MATLAB tools used in this study are open source and freely available online: https://oss.deltares.nl/web/delft3d. The Delft3D Suite was developed by Deltares with the main office located at Rotterdamseweg 185, 2629 HD, Delft, The Netherlands. Contact can be made through the contact form (https://oss.deltares.nl/web/delft3d/contact) or via the sales department with the following email and contact number: sales@deltaressystems.nl, +31 (0)88 335 8188. The Delft3D flow (FLOW), morphology (MOR) and waves (WAVE) modules were first made available in 2011 and is written using Fortran and C/C++ language rules (Lesser, 2009).

The running of the model requires the use of MATLAB versions 2013 or higher. This software can be attained through purchase, student version or trial online: https://nl.mathworks.com/products/matlab.html. Contact can be made to MathWorks, the developer, through its representative in the Netherlands (Dr. Holtroplaan 5B, Phone: +31-40-2156700) or via the corporate headquarters. The sources of all datasets and parameter values used for the model developed have been provided in the Methods section and in Appendix A of the paper. Additionally, the typical input files for the setup of the base model along with the plant growth script have been provided in the ***Supplemental Materials***. With regards to the hardware required, a standard PC with minimum 8 GB RAM.

Acknowledgements

I would first like to express my gratitude to the staff of Coastal and Port Development Department of IHE Delft Institute for Water education and Deltares who have been instrumental in shaping the framework for this research and generously gave of their time and efforts. P.W.J.M.Willemsen was supported by the research programme BE SAFE (NWO; 850.13.010), financed primarily by the Netherlands Organisation for Scientific Research (NWO; 850.13.012). This research did not receive any specific grant from funding agencies in the public, commercial, or not-for-profit sectors.

Appendix A. Supplementary data

Supplementary data related to this article can be found at https://doi.org/10.1016/j.envsoft.2018.08.004.

References

Airoldi, L., Abbiati, M., Beck, M.W., Hawkins, S.J., Jonsson, P.R., Martin, D., Moschella, P.S., Sundelöf, A., Thompson, R.C., Åberg, P., 2005. An ecological perspective on the deployment and design of low-crested and other hard coastal defence structures. Coast. Eng. 52, 1073–1087.

Allen, J.R., 2000. Morphodynamics of Holocene salt marshes: a review sketch from the Atlantic and southern North Sea coasts of Europe. Quat. Sci. Rev. 19, 1155–1231.

Attema, Y., 2014. Long-term Bio-geomorphological Modelling of the Formation and Succession of Salt Marshes. TU Delft, Delft University of Technology.

Balke, T., Webb, E.L., den Elzen, E., Galli, D., Herman, P.M., Bouma, T.J., 2013. Seedling establishment in a dynamic sedimentary environment: a conceptual framework using mangroves. J. Appl. Ecol. 50, 740–747.

Baptist, M., Babovic, V., Rodríguez Uthurburu, J., Keijzer, M., Uittenbogaard, R., Mynett, A., Verwey, A., 2007. On inducing equations for vegetation resistance. J. Hydraul. Res. 45, 435–450.

Bendoni, M., Mel, R., Solari, L., Lanzoni, S., Francalanci, S., Oumeraci, H., 2016. Insights into lateral marsh retreat mechanism through localized field measurements. Water Resour. Res. 52, 1446–1464.

Borsje, B.W., van Wesenbeeck, B.K., Dekker, F., Paalvast, P., Bouma, T.J., van Katwijk, M.M., de Vries, M.B., 2011. How ecological engineering can serve in coastal protection. Ecol. Eng. 37, 113–122. https://doi.org/10.1016/j.ecoleng.2010.11.027.

Bouma, T., van Belzen, J., Balke, T., van Dalen, J., Klaassen, P., Hartog, A., Callaghan, D., Hu, Z., Stive, M., Temmerman, S., 2016. Short-term mudflat dynamics drive long--term cyclic salt marsh dynamics. Limnol. Oceanogr. 61, 2261–2275.

Bouma, T., Vries, M.D., Low, E., Kusters, L., Herman, P., Tanczos, I., Temmerman, S., Hesselink, A., Meire, P., Van Regenmortel, S., 2005. Flow hydrodynamics on a mudflat and in salt marsh vegetation: identifying general relationships for habitat characterisations. Hydrobiologia 540, 259–274.

Cheon, S.-H., Suh, K.-D., 2016. Effect of sea level rise on nearshore significant waves and coastal structures. Ocean Eng. 114, 280–289. https://doi.org/10.1016/j.oceaneng.2016.01.026.

Clough, J., Polaczyk, A., Propato, M., 2016. Modeling the potential effects of sea-level rise on the coast of New York: integrating mechanistic accretion and stochastic uncertainty. Environ. Model. Software 84, 349–362.

Cowell, P.J., Thom, B.G., 1995. Morphodynamics of coastal evolution. In: Carter, R.W.G., Woodroffe, C.D. (Eds.), Coastal Evolution: Late Quaternary Shoreline Morphodynamics, pp. 33–86.

Craft, C., Clough, J., Ehman, J., Joye, S., Park, R., Pennings, S., Guo, H., Machmuller, M., 2009. Forecasting the effects of accelerated sea-level rise on tidal marsh ecosystem services. Front. Ecol. Environ. 7, 73–78.

Crosby, S.C., Sax, D.F., Palmer, M.E., Booth, H.S., Deegan, L.A., Bertness, M.D., Leslie, H.M., 2016. Salt marsh persistence is threatened by predicted sea-level rise.

Estuarine. Coastal and Shelf Science 181, 93–99.
Deltares, 2014. Delft3D, Functional Specifications Functional Specifications Deltares, Boussinesqweg 1, 2629 HV Delft, P.O. Box 177, 2600 MH Delft, The Netherlands.
Dijkstra, J.T., 2008. How to Account for Flexible Aquatic Vegetation in Large-scale Morphodynamic ModelsInternational Conference on Coastal Engineering. pp. 2820–2831.
Fagherazzi, S., Kirwan, M.L., Mudd, S.M., Guntenspergen, G.R., Temmerman, S., D'Alpaos, A., Koppel, J., Rybczyk, J.M., Reyes, E., Craft, C., 2012. Numerical models of salt marsh evolution: ecological, geomorphic, and climatic factors. Rev. Geophys. 50.
Horton, B.P., Rahmstorf, S., Engelhart, S.E., Kemp, A.C., 2014. Expert assessment of sea-level rise by AD 2100 and AD 2300. Quat. Sci. Rev. 84, 1–6.
Hu, K., Ding, P., Wang, Z., Yang, S., 2009. A 2D/3D hydrodynamic and sediment transport model for the Yangtze Estuary, China. J. Mar. Syst. 77, 114–136. https://doi.org/10.1016/j.jmarsys.2008.11.014.
Hu, Z., Wang, Z.B., Zitman, T.J., Stive, M.J., Bouma, T.J., 2015. Predicting long-term and short-term tidal flat morphodynamics using a dynamic equilibrium theory. J. Geophys. Res.: Earth Surface 120, 1803–1823.
Hydraulics, W.D., 2002. DELFT3D-WAVE User Manual Version 2.01. WL Delft Hydraulics, Delft, The Netherlands.
IPCC, 2013. The 5th Assessment Report. New York.
Kirwan, M.L., Megonigal, J.P., 2013. Tidal wetland stability in the face of human impacts and sea-level rise. Nature 504, 53–60.
Kirwan, M.L., Mudd, S.M., 2012. Response of salt-marsh carbon accumulation to climate change. Nature 489, 550–553.
Kirwan, M.L., Temmerman, S., Skeehan, E.E., Guntenspergen, G.R., Fagherazzi, S., 2016. Overestimation of marsh vulnerability to sea level rise. Nat. Clim. Change 6, 253.
Lesser, G.R., 2009. An Approach to Medium-term Coastal Morphological Modelling UNESCO-IHE. Institute for Water Education.
Li, F., Van Gelder, P., Ranasinghe, R., Callaghan, D., Jongejan, R., 2014. Probabilistic modelling of extreme storms along the Dutch coast. Coast Eng. 86, 1–13.
Lokhorst, I., 2016. Effects of Mud, Spartina Anglica and Zostera Marina on Large Scale Morphodynamics in a Tide-dominated Estuary.
Maan, D., Prooijen, B., Wang, Z., De Vriend, H., 2015. Do intertidal flats ever reach equilibrium? J. Geophys. Res.: Earth Surface 120, 2406–2436.
MacVean, L.J., Lacy, J.R., 2014. Interactions between waves, sediment, and turbulence on a shallow estuarine mudflat. J. Geophys. Res.: Oceans 119, 1534–1553.
Mariotti, G., Fagherazzi, S., 2010. A numerical model for the coupled long-term evolution of salt marshes and tidal flats. J. Geophys. Res.: Earth Surface 115.
Monden, M., 2010. Modeling the Interaction between Morphodynamics and Vegetation in the Nisqually River Estuary. Delft (MSc Thesis Report).
Morris, J.T., Sundareshwar, P., Nietch, C.T., Kjerfve, B., Cahoon, D.R., 2002. Responses of coastal wetlands to rising sea level. Ecology 83, 2869–2877.
Mudd, S.M., D'Alpaos, A., Morris, J.T., 2010. How does vegetation affect sedimentation on tidal marshes? Investigating particle capture and hydrodynamic controls on biologically mediated sedimentation. J. Geophys. Res.: Earth Surface 115.
Mudd, S.M., Fagherazzi, S., 2016. 12 Salt Marsh Ecosystems: Tidal Flow, Vegetation, and Carbon Dynamics. A Biogeoscience Approach to Ecosystems: 407.
Nyman, J.A., Walters, R.J., Delaune, R.D., Patrick, W.H., 2006. Marsh vertical accretion via vegetative growth. Estuar. Coast Shelf Sci. 69, 370–380.
Oorschot, Mv, Kleinhans, M., Geerling, G., Middelkoop, H., 2016. Distinct patterns of interaction between vegetation and morphodynamics. Earth Surf. Process. Landforms 41, 791–808.
Rahman, A., 2015. Cliff Erosion of Salt Marshes.
Roelvink, D., 2011. A Guide to Modeling Coastal Morphology World Scientific.
Roelvink, J., 2006. Coastal morphodynamic evolution techniques. Coast Eng. 53, 277–287.
Schepers, L., Kirwan, M., Guntenspergen, G., Temmerman, S., 2017. Indicators of Marsh Vulnerability to Sea Level Rise Neglect Lateral Runaway Erosion. Spatial Patterns and Bio-geomorphological Effects of Vegetation Loss in a Submerging Coastal Marsh: 81.
Schile, L.M., Callaway, J.C., Morris, J.T., Stralberg, D., Parker, V.T., Kelly, M., 2014. Modeling tidal marsh distribution with sea-level rise: evaluating the role of vegetation, sediment, and upland habitat in marsh resiliency. PLoS One 9 e88760.
Schwarz, C., Ye, Q., Wal, D., Zhang, L., Bouma, T., Ysebaert, T., Herman, P., 2014. Impacts of salt marsh plants on tidal channel initiation and inheritance. J. Geophys. Res.: Earth Surface 119, 385–400.
Schwarz, C., Ysebaert, T., Zhu, Z., Zhang, L., Bouma, T.J., Herman, P.M., 2011. Abiotic factors governing the establishment and expansion of two salt marsh plants in the Yangtze Estuary, China. Wetlands 31, 1011–1021.
Schwimmer, R.A., 2001. Rates and processes of marsh shoreline erosion in Rehoboth Bay, Delaware, USA. J. Coast Res. 672–683.
Sistermans, P., Nieuwenhuis, O., 2004. Western scheldt estuary (the Netherlands) Eurosion Case.
Stark, J., Meire, P., Temmerman, S., 2017. Changing tidal hydrodynamics during different stages of eco-geomorphological development of a tidal marsh: a numerical modeling study. Estuar. Coast Shelf Sci. 188, 56–68.
Stocker, T., 2014. Climate Change 2013: the Physical Science Basis: Working Group I Contribution to the Fifth Assessment Report of the Intergovernmental Panel on Climate Change. Cambridge University Press.
Stralberg, D., Brennan, M., Callaway, J., Wood, J., Schile, L., 2011. Evaluating Tidal Marsh Sustainability in the Face of Sea-level Rise: a Hybrid.
Sweet, W.V., Kopp, R.E., Weaver, C.P., Obeysekera, J., Horton, R.M., Thieler, E.R., Zervas, C., 2017. Global and regional sea level rise scenarios for the United States.
Temmerman, S., Bouma, T., Govers, G., Wang, Z., De Vries, M., Herman, P., 2005. Impact of vegetation on flow routing and sedimentation patterns: three-dimensional modeling for a tidal marsh. J. Geophys. Res.: Earth Surface 110.
Temmerman, S., Bouma, T., Van de Koppel, J., Van der Wal, D., De Vries, M., Herman, P., 2007. Vegetation causes channel erosion in a tidal landscape. Geology 35, 631–634.
Temmerman, S., Govers, G., Meire, P., Wartel, S., 2003. Modelling long-term tidal marsh growth under changing tidal conditions and suspended sediment concentrations, Scheldt estuary, Belgium. Mar. Geol. 193, 151–169.
Temmerman, S., Govers, G., Wartel, S., Meire, P., 2004. Modelling estuarine variations in tidal marsh sedimentation: response to changing sea level and suspended sediment concentrations. Mar. Geol. 212, 1–19.
Temmerman, S., Meire, P., Bouma, T.J., Herman, P.M., Ysebaert, T., De Vriend, H.J., 2013. Ecosystem-based coastal defence in the face of global change. Nature 504, 79–83.
Temmerman, S., Vandenbruwaene, W., Biermans, G., Meire, P., Bouma, T., Klaasse, P., Balke, T., Callaghan, D., de Vries, M., van Steeg, P., 2010. Flow Interaction with Patchy Dynamic Vegetation: Implications for Bio-geomorphic Evolution of Coastal WetlandsProc Hydralab III Joint User Meeting.
Thampanya, U., Vermaat, J.E., Sinsakul, S., Panapitukkul, N., 2006. Coastal erosion and mangrove progradation of Southern Thailand. Estuar. Coast Shelf Sci. 68, 75–85. https://doi.org/10.1016/j.ecss.2006.01.011.
Thorne, K.M., Elliott-Fisk, D.L., Wylie, G.D., Perry, W.M., Takekawa, J.Y., 2014. Importance of biogeomorphic and spatial properties in assessing a tidal salt marsh vulnerability to sea-level rise. Estuar. Coast 37, 941–951.
Tonelli, M., Fagherazzi, S., Petti, M., 2010. Modeling wave impact on salt marsh boundaries. J. Geophys. Res.: Oceans 115.
Townend, I., Fletcher, C., Knappen, M., Rossington, K., 2011. A review of salt marsh dynamics. Water Environ. J. 25, 477–488.
Trenhaile, A.S., 2009. Modeling the erosion of cohesive clay coasts. Coast Eng. 56, 59–72. https://doi.org/10.1016/j.coastaleng.2008.07.001.
Turner, R.E., Swenson, E.M., Milan, C.S., Lee, J.M., Oswald, T.A., 2004. Below-ground biomass in healthy and impaired salt marshes. Ecol. Res. 19, 29–35.
Van der Wegen, M., Jaffe, B., Foxgrover, A., Roelvink, D., 2016. Mudflat morphodynamics and the impact of sea level rise in south san Francisco Bay. Estuar. Coast 1–13. https://doi.org/10.1007/s12237-016-0129-6.
Van der Wegen, M., Jaffe, B., Foxgrover, A., Roelvink, D., 2017. Mudflat morphodynamics and the impact of sea level rise in south san Francisco Bay. Estuar. Coast 40, 37–49.
Van der Wegen, M., Roelvink, J., 2008. Long-term morphodynamic evolution of a tidal embayment using a two-dimensional, process-based model. J. Geophys. Res.: Oceans 113.
van Loon-Steensma, J.M., 2015. Salt marshes to adapt the flood defences along the Dutch Wadden Sea coast. Mitig. Adapt. Strategies Glob. Change 20, 929–948. https://doi.org/10.1007/s11027-015-9640-5.
van Maanen, B., Coco, G., Bryan, K.R., 2015. On the Ecogeomorphological Feedbacks that Control Tidal Channel Network Evolution in a Sandy Mangrove SettingProc R Soc a the Royal Society. 20150115.
Vuik, V., Jonkman, S.N., 2016. Wave Attenuation by Salt Marsh Vegetation18th Physics of Estuaries and Coastal Seas Conference, 2016.
Vuik, V., Jonkman, S.N., Borsje, B.W., Suzuki, T., 2016. Nature-based flood protection: the efficiency of vegetated foreshores for reducing wave loads on coastal dikes. Coast. Eng. 116, 42–56.
Willemsen, P., Horstman, E., Borsje, B., Friess, D., Dohmen-Janssen, C., 2016. Sensitivity of the sediment trapping capacity of an estuarine mangrove forest. Geomorphology 273, 189–201.
Winterwerp, J.C., Erftemeijer, P.L.A., Suryadiputra, N., van Eijk, P., Zhang, L., 2013. Defining eco-morphodynamic requirements for rehabilitating eroding mangrove-mud coasts. Wetlands 33, 515–526. https://doi.org/10.1007/s13157-013-0409-x.
Ye, Q., 2012. An Approach towards Generic Coastal Geomorphological Modelling with Applications TU Delft. Delft University of Technology.
Zhou, Z., Ye, Q., Coco, G., 2016. A one-dimensional biomorphodynamic model of tidal flats: sediment sorting, marsh distribution, and carbon accumulation under sea level rise. Adv. Water Resour. 93, 288–302.